Physicochemical functionality of chimeric isomaltomegalosaccharides with α-(1→4)-glucosidic segments of various lengths

Weeranuch Lang[1,*], Yuya Kumagai[1], Shinji Habu[1], Juri Sadahiro[1], Takayoshi Tagami[1], Masayuki Okuyama[1], Shinichi Kitamura[2], Nobuo Sakairi[3], Atsuo Kimura[1,*]

[1]Research Faculty of Agriculture, Hokkaido University, Sapporo 060-8589, Japan

[2]Center for Research and Development of Bioresources, Organization for Research Promotion, Osaka Prefecture University, Osaka 599-8531, Japan

[3]Graduate School of Environmental Science, Hokkaido University, Sapporo 060-0810, Japan

[*]Corresponding author: tel/fax, +81 11 706 2808; e-mail address, weranuch@abs.agr.hokudai.ac.jp (Weeranuch Lang) and kimura@abs.agr.hokudai.ac.jp (Atsuo Kimura)

Abbreviations: DDase, dextran dextrinase; DP, average value of degree of polymerization; G*n*, maltodextrin with DP = *n*; IMS, isomaltomegalosaccharide; IMS-*p*/*q* (e.g., IMS-15/9), IMS with DPs of *p* and *q* for α-(1→6)- and α-(1→4)-segments, respectively; K_c, stability constant; K_s, equilibrium constant; MWCO-2000 and MWCO-3500, dialysis tubes with molecular weight cutoffs of 2,000 and 3,500, respectively; QC, quercetin; Q3G, quercetin-3-*O*-β-glucoside; TDT; thermal decomposition temperature; TGA, thermogravimetric analysis; TNS, 2-*p*-toluidinylnaphthalene-6-sulfonate.

Abstract

Isomaltomegalosaccharide (IMS) is a long chimeric glucosaccharide composed of α-(1→6)- and α-(1→4)-linked segments at nonreducing and reducing ends, respectively; the hydrophilicity and hydrophobicity of these segments are expected to lead to bifunctionality. We enzymatically synthesized IMS with average degrees of polymerization (DPs) of 15.8, 19.3, and 23.5, where α-(1→4)-segments had DPs of 3, 6, and 9, respectively. IMS exhibited considerably higher water solubility than maltodextrin because of the α-(1→6)-segment and an identical resistance to thermal

degradation as short dextran. Interaction of IMS with a fluorescent probe of 2-*p*-toluidinylnaphthalene-6-sulfonate demonstrated that IMS was more hydrophobic than maltodextrin, where the degree of hydrophobicity increased as DP of α-(1→4)-segment increased (9 > 6 > 3). Fluorescent pyrene-estimating polarity of IMS was found to be similar to that of methanol or 1-butanol. The bifunctional IMS enhanced the water solubility of quercetin-3-*O*-glucoside and quercetin: the solubilization of less-soluble bioactive substances is beneficial in carbohydrate industry.

Keywords: dextran dextrinase, isomaltomegalosaccharide, chimeric structure, bifunctionality, quercetin flavonoid, water solubility enhancement

1. Introduction

Glucosaccharides, such as soluble starch and dextran, are hydrophilic due to the presence of numerous surface hydroxyl groups that promote water solubility. Monosaccharide glucose containing methine groups has a negligibly weak hydrophobicity. However, α-(1→4)-glucosaccharides (i.e., maltodextrin and cyclodextrin) exhibit high hydrophobicity arising from stereochemical constrained chains with helical structures (Balasubramanian et al., 1993), whereby the internal surface is relatively apolar because all the methine groups point inwards. The degree of apolarity of the sugar chain can be evaluated by hydrophobic interaction with fluorophore probe 2-*p*-toluidinylnaphthalene-6-sulfonate (TNS) (Das et al., 1995) because the emission intensity of TNS is higher in a nonpolar state (i.e., in sugar chain) than in an aqueous state. TNS interacts with the helical chain of maltodextrin where this α-(1→4)-glucosaccharide forms a helical conformation for degrees of polymerization (DPs) greater than 5 and an incipient helix-type structure for lower DPs (Sundari et al., 1991; Aoyama et al., 1992). By contrast, dextran composed of sole α-(1→6)-glucosyl units possesses no hydrophobicity since this α-(1→6)-glucosaccharide does not affect the fluorescence of TNS (Sundari & Balasubramanian, 1997), indicating that dextran is a hydrophilic saccharide. Functional properties are affected by the type and length of glucosaccharide chains. In this study, we hypothesize that a glucosaccharide containing both α-(1→4)- and α-(1→6)-glucosidic segments ["chimeric" saccharide; i.e., isomaltomegalosaccharide

(IMS)] (Lang et al., 2022) could exhibit the bifunctionality, that is, both hydrophobicity and hydrophilicity.

Dextran dextrinase (DDase; EC 2.4.1.2) is a glucosyltransferase that catalyzes a two-substrate reaction with maltodextrins as the substrates. DDase can cleave an α-(1→4)-linkage at the nonreducing end of a donor substrate and transfer the glucosyl unit to the nonreducing end of an acceptor substrate to generate an α-(1→6)- or α-(1→4)-linkage (Yamamoto et al., 1992). Consecutive transfers from the α-(1→4)-linkage result in the extension of the α-(1→6)-linked segment, whereby the enzyme finally synthesizes a macromolecule of viscous dextran (Yamamoto et al., 1993). Theoretically, the dextran produced by DDase is not an α-(1→6)-glucan because the reducing terminal region is composed of α-(1→4)-linkages originating from maltodextrin of the acceptor substrate, implying the product is a "chimeric" polysaccharide with α-(1→6)- and α-(1→4)-linked segments. Recently, we found that intermediate-sized saccharides could be effectively produced by DDase from *Gluconobacter oxydans* ATCC 11894 under optimized conditions (Lang et al., 2022). The product is called an IMS based on the definition of a megalosaccharide (Thoma et al., 1959), for which the DP ranges between that of an oligosaccharide (DP = 2–9) and a polysaccharide. The DP of a polysaccharide is not well-defined, but the properties of polysaccharides emerge for DPs of more than 100 or 200 (Kitamura S, personal information); thus, the DP of a megalosaccharide is considered to be 10–100 (or 100–200). The IMS is a chimeric saccharide comprised of α-(1→6)- and α-(1→4)-segments, where the α-(1→4)-segment is derived from a maltodextrin substrate. The IMS is expected to possess a low viscosity and a high water solubility because the linear α-(1→6)-segment promotes hydrophilicity, as suggested by Sundari et al. (1991) and Balasubramanian et al. (1993). An *in vivo* study was performed to investigate the functionality of IMS. The IMS with short α-(1→4)-segment enhanced the absorption of quercetin-3-*O*-β-glucoside (Q3G) in the rat small intestine (Shinoki et al., 2013). In addition, higher enzymatic degradation of an azobenzene dye (ethyl red, an environmental pollutant) by azoreductase occurred in the presence of an IMS than in the presence of β-cyclodextrin possibly because of weak hydrophobic interaction between the IMS and ethyl red (Lang et al., 2014). Strong interaction of β-cyclodextrin–ethyl red complex inhibited enzymic degradation by its steric hindrance. Recently, an IMS was reported to enhance the barrier function of

intestinal epithelial tight junctions, which could facilitate inflammation suppression and reduce the risks of chronic diseases (Hara et al., 2017).

In this study, we revealed the bifunctionality of the chimeric IMS with α-(1→4)-segments of various lengths: i.e., three IMSs with DPs of 15.8, 19.3, and 23.5 (IMS-13/3, IMS-13/6, and IMS-15/9, respectively) (Fig. 1). Fluorescence studies were performed to determine the hydrophobic characteristics of the IMS substrates: TNS was used to determine the stability constants (K_cs), and the sense of polarity was determined using polycyclic aromatic pyrene; to the best of our knowledge, the sense of polarity was determined for the first time for carbohydrates in this study. The IMS-induced water solubilization of Q3G and quercetin (QC) (which are bioactive flavonoids that are widely used as health supplements) was also evaluated using a phase solubility diagram. The hydrophobicity of IMS facilitates the aqueous solubilization of these flavonoids. Properties related to the α-(1→6)-segment (water solubility and thermal stability) were analyzed.

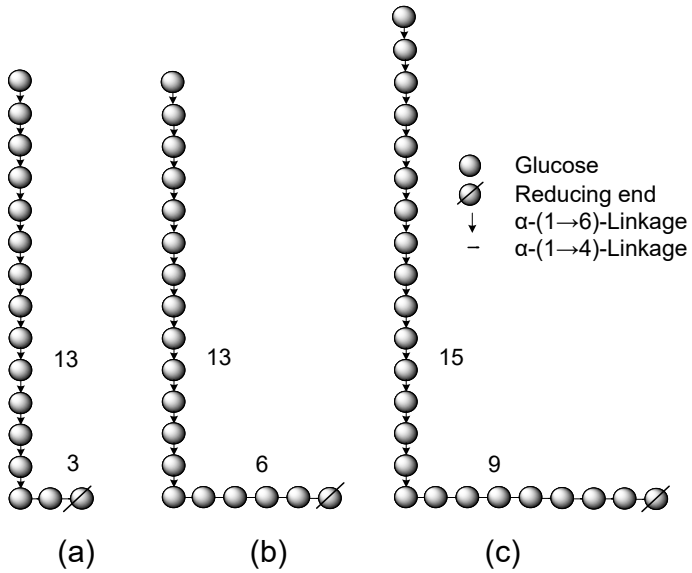

Fig. 1. Proposed structure of isomaltomegalosaccharide (IMS); a, IMS-13/3; b, IMS-13/6; c, IMS-15/9; numbers, DPs (average values) of α-(1→6)- and α-(1→4)-segments.

2. Materials and methods

2.1. Materials

Q3G and QC hydrate were purchased from Extrasynthese (Cedex, France) and Tokyo Chemical Industry (Tokyo, Japan), respectively. Dextran T1 (DP = 7), T1.5 (DP = 10), and T3.5 (DP

= 20) were obtained from Pharmacosmos (Holbaek, Denmark). Dextran T10 (DP = 60) and T40 (DP = 250) were purchased from Amersham Biosciences (Uppsala, Sweden). Amylose (DP = 28 and DP = 600; synthetic products) was purchased from Glico Nutrition (Osaka, Japan). Amylose (DP = 18; corn) was purchased from Hayashibara (Okayama, Japan). TNS was obtained from Sigma–Aldrich (Shinagawa, Japan). Pyrene, polar protic solvents, and polar aprotic solvents were purchased from Nacalai Tesque (Kyoto, Japan). Cellulose dialysis membranes [with molecular weight cutoffs of 2,000 (MWCO-2000) and 3,500 (MWCO-3500)] were purchased from Spectrum (Rancho Dominguez, CA, USA). Maltotriose (G3) and G6/G7 (maltohexaose and maltoheptaose; commercial product Fugioligo) were donated by Nihon Shokuhin Kako (Tokyo, Japan). Maltodextrin with average DP = 11.8 (G12), of which DP ranged in 11.2–13.6 (see Fig. 2C), was prepared by the hydrolysis of short amylose (DP = 16.5–19.5; Carbosynth, Berkshire, UK) as follows (Fig. S1): short amylose (100 mg/mL) was suspended in a 50 mM sodium acetate buffer (pH 5.0) containing 0.02% sodium azide and treated with recombinant pullulanase (5 μL/mL; Sigma–Aldrich, St. Louis, MO, USA) at 37 °C for 2 d to cleave the α-(1→6)-linkage; the G12 fraction was then isolated by precipitation with 75% (v/v) methanol and dried *in vacuo* (45% yield). The ^{1}H-NMR analysis of isolated G12 is shown in Fig. S2A and S2B.

2.2. Preparation of freeze-dried DDase

Cultivation of *G. oxydans*, extracellular DDase preparation, and enzyme activity assays were performed according to methods previously used (Lang et al., 2022). Suitable quantities of cells were suspended in a 25 mM sodium acetate buffer (pH 4.2, 50 mL) containing 1% G3 and incubated at 30 °C for 3 h under agitation at 200 rpm (rev/min). During incubation of the cells with G3, DDase was secreted extracellularly and produced dextran from G3, which was tightly bound to DDase (dextran-bound DDase) (Lang et al., 2022). The resultant dextran-bound enzyme was dialyzed against water containing 0.02% sodium azide at 4 °C for 2 d and then frozen at -80 °C. Dried DDase was obtained by freeze-drying for 2 d using a lyophilizer FDU-1200 (Eyela, Tokyo, Japan).

2.3. Production and structural analysis of IMS

As previously reported (Lang et al., 2022), increasing the substrate concentration promoted IMS formation and depressed dextran formation, and increasing the agitation efficiency increased the α-(1→6)-linkage content of IMS and decreased dextran formation. Freeze-dried DDase (0.1 U/mL) was mixed with 200 mM G3, G4, G6/G7 or G12 containing a 50 mM sodium acetate buffer (pH 4.2), where the reaction volume was 40 mL, and incubated at 50 °C for 96 h in a 200-mL baffled flask under agitation at 100 rpm. An appreciable quantity of the mixture (100–200 μL) was recovered at the designated time. The reaction was terminated by heating at 100 °C for 20 min, followed by centrifugation at 12,000× *g* for 10 min at 4 °C to remove the denatured enzyme. The progress of the formation of the α-(1→6)-linkage of saccharides contained in the reaction mixture was monitored using ^{1}H-NMR according to a method we have previously reported (Lang et al., 2022).

The reaction was allowed to proceed for 96 h, after which IMS and dextran were separated by methanol fractionation based on a procedure we have previously reported (Lang et al., 2022), except that 50% (v/v) methanol was used to precipitate the dextran generated from G3 or G4. The IMSs obtained from G6/G7 and G12 were further purified by dialysis with MWCO-2000 and MWCO-3500, respectively, for 18 h at 4 °C. The IMSs were desalted using an ion exchange resin (Lang et al., 2014). The IMS obtained from G6/G7 was treated with porcine pancreatic α-amylase (Sigma–Aldrich) to shorten the length of the reducing terminal α-(1→4)-segment (Lang et al., 2022). The carbohydrate concentration was measured by the phenol–sulfuric acid method (Dubois et al., 1959) using a glucose standard. Both the average value of DP and type of α-glucosyl linkage of the IMSs were analyzed by ^{1}H-NMR (Lang et al., 2014) (Fig. S2C and S2D). The saccharide size distribution was estimated using gel permeation HPLC (Lang et al., 2022). According to our previous method (Lang et al., 2022), the length of α-(1→4)-chain of IMS was investigated by digestion with dextran glucosidase, which catalyzes the exo-wise hydrolysis of α-(1→6)-glucosidic linkage of substrate at nonreducing end and no attack on α-(1→4)-glucosidic linkage (Saburi et al., 2006), and the formed maltodextrins were analyzed. Water content of IMS is shown in Table S1.

2.4. Thermal properties and water solubility

The thermal decomposition of the IMSs was measured with a thermogravimetric analysis (TGA) apparatus (TG 8120; Rigaku, Tokyo, Japan). An aluminum crucible was used to hold 10 mg of an oven-dried sample at 40 °C for 1 d. TGA was performed by elevating the temperature from 50 to 500 °C at a heating rate of 10 °C/min under an N_2 atmosphere with a flow rate of 50 mL/min. The data were analyzed using the Thermo plus EVO version 2.060-1 software program (Rigaku).

Water solubility was determined by dissolving the IMS sample (40 mg) in 0.1 mL of water using a 1.5-mL microcentrifuge tube. The liquid in the tube was mixed thoroughly and left to stand at 25 °C for 5 h. The suspension was centrifuged at 12,000× g at 25 °C for 20 min. The supernatant (50 μL) was lyophilized and weighed, and the results were used to calculate the dissolved quantity of the sample in 1 mL of water. Commercial samples of three amyloses and four dextrans were analyzed in the same way.

2.5. TNS binding analysis

Fluorescence titration was conducted to investigate the formation of complexes between 0–10 mM IMS and 10 μM TNS in water on a Hitachi F-4500 spectrometer (Tokyo, Japan) at an excitation wavelength of 360 nm according to a previously reported method (Buranaboripan et al., 2014). K_c was determined from Benesi–Hildebrand plots [Eq. (1)] at an emission intensity of 447 nm for IMS-13/3 and IMS-13/6 and 467 nm for IMS-15/9.

$$1/(I - I_0) = 1/(I' - I_0) + 1/\{K_c(I' - I_0)[H]\} \quad (1)$$

In the equation above, I_0, I and I' are the initial fluorescence intensities of TNS without saccharide, with saccharide of different concentrations ([H]), and with saccharide at the maximum concentration, respectively.

2.6. Polarity estimated by pyrene

Ten μL pyrene in ethanol was added to saccharide in water (final volume, 1 mL), and then the fluorescence spectra were immediately monitored at 25 °C on a Hitachi F-4500 spectrometer at an excitation wavelength of 335 nm, where the ratio of the emission intensity at 375 nm (I_1) to that at 384 nm (I_3) was estimated. Final concentrations of pyrene, saccharide, and ethanol were 0.5 μM, 20–100

mM, and 1% (v/v), respectively. The I_1/I_3 value of 1% (v/v) ethanol solution was measured to be 1.4. The same approach was applied to estimate the I_1/I_3 values of polar protic solvents (e.g., methanol) and polar aprotic solvents (e.g., dimethyl sulfoxide). The determined I_1/I_3 values and dielectric constants for the solvents (https://macro.lsu.edu/howto/solvents/Dielectric%20Constant%20.htm) were used to generate calibration curves (see Fig. 3D) to evaluate the polarities of the IMSs and dextrans.

2.7. Phase solubility of flavonoids

An excess quantity of Q3G or QC (1.0 mg) was mixed with 100 μL of an aqueous solution containing 0–40 mM saccharide. The suspension was mixed frequently, left to stand at 25 °C for 6 h, and a solution saturated with Q3G or QC was recovered using a previously reported approach (Lang et al., 2014). A portion of the saturated solution was diluted with dimethyl sulfoxide and used to quantify the flavonoid by measuring the absorbance at 360 nm. The apparent equilibrium constant (K_s) was estimated from the phase solubility diagram (Higuchi and Connors, 1965) according to a method we have previously reported (Lang et al., 2014).

3. Results and discussion

3.1 Production of IMSs with α-(1→4)-segments of various lengths at the reducing end

G. oxydans DDase, a cell surface protein, is secreted from cells when starch hydrolysate (maltodextrin or glucose) is present in the medium (Suzuki et al., 1999; Sadahiro et al., 2015; Lang et al., 2022). Cultivation of cells with maltodextrin (except G2) results in the extracellular generation of dextran-bound DDase, which is more thermostable than the dextran-free enzyme (Lang et al., 2022). It is also known that coexistence with dextran stabilizes the activities of freeze-dried enzymes (Allison et al., 1998; Anchordoquy et al., 2001), suggesting that dextran-bound DDase maintains its activity after freeze-drying and can be stored for long periods. Dextran-bound DDase (0.127 U/mL) was obtained from the medium in which cells (corresponding to 31.5 mg dry cells) were treated with 1.0% G3. The enzyme maintained 94% of its original activity after lyophilization, which makes extended storage of dextran-bound DDase feasible.

A 200 mM substrate (G3, G4, G6/G7, or G12) was reacted with 0.1 U/mL freeze-dried DDase for 96 h according to our previous approach (Lang et al., 2022), except that the incubation temperature was increased from 45 °C to 50 °C, without affecting the IMS production yield. Incubation at 50 °C decreased the viscosity of the reaction mixture containing the highly concentrated (200 mM) substrate and encumbered the retrogradation of G12. Long maltodextrin G12 immediately thickened to form a gel at a lower temperature.

We recovered the reaction mixture at the indicated time, and all the saccharides contained in the reaction mixture (remaining substrate and formed products) were subjected to ^{1}H-NMR monitoring (Fig. 2A). The degree of formation of the α-(1→6)-linkage increased in a sigmoidal manner due to α-(1→4)-linkage formation by DDase (Lang et al., 2022). Table 1 shows that L_{max} [the maximum α-(1→6)-linkage content of all the saccharides] increased from 56.7 to 66.3% for G3–G6/G7 as the DP of the substrate increased. The L_{max} value of G12 (62.7%) is an exception of this manner since highly concentrated G12 (200 mM) gradually retrograded during the long reaction, even at 50 °C. The reaction time (T_{50}) at which half of L_{max} was obtained increased in the order G12 > G6/G7 > G4 > G3 (Table 1), indicating that α-(1→6)-linkage formation was slower for a longer substrate.

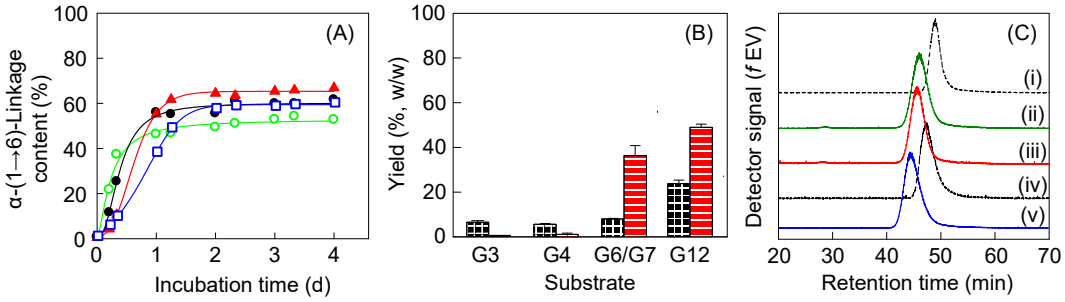

Fig. 2. Production of isomaltomegalosaccharide (IMS). **A**, Increase in the α-(1→6)-linkage content of all saccharides in the reaction mixture. ○, G3; ●, G4; ▲, G6/G7; □, G12. **B**, Yield of dextran (black) and IMS (red) isolated from the reaction mixture for a 96-h reaction time. Yield (%; w/w), amount of each product per that of substrate used. **C**, Size distribution of IMS (ii, iii, or v) and substrate (i or iv). i, G6/G7; ii, IMS-13/3; iii, IMS-13/6; iv, G12; v, IMS-15/9.

Table 1. Formation of α-(1→6)-linkages in saccharides in the reaction mixture and characterization of the isomaltomegalosaccharide (IMS) fraction.

200 mM Substrate	All saccharides in reaction mixture		Isolated IMS		
	L_{max}[a] (%)	T_{50}[b] (h)	DP	α-(1→6)-content (%)	DP of two chains[c]
G3	56.7	5.9	NO	NO	NO
G4	61.1	9.8	13.2	70.3	4: 9
G6/G7	66.3	14.3	19.3	69.3	6: 13
G12	62.6	18.0	23.5	63.2	9: 15

[a] Maximal α-(1→6)-linkage content of all saccharides.

[b] Reaction time at which half of L_{max} was obtained.

[c] The first and second values denote the DPs of the α-(1→4)- and α-(1→6)-segments, respectively. NO was not obtained because of a low IMS yield from G3.

The subsequent DDase reaction at 96 h showed that an adequate content of α-(1→6)-segment was generated for each substrate (Fig. 2A); therefore, the product was separated into IMS and dextran by methanol fractionation. The IMSs from G6/G7 and G12 were subjected to further purification by dialysis using MWCO-2000 and MWCO-3500, respectively, to remove saccharide components with DPs below 12 and 22, respectively. Fig. 2B shows the yield of purified IMS or dextran (w/w, as a percentage of the initial quantity of substrate), demonstrating that the production of both IMS and dextran increases with the DP of the maltodextrin substrates. IMSs were obtained in a high yield from the reaction of G6/G7 and G12 (36 and 49%, respectively) but in a very low yield from the reaction of G3 and G4 (0.04 and 0.21%, respectively), where the main products were oligosaccharides. Even for a small yield, the IMS from G4 had a DP of 13.2, as analyzed by ^{1}H-NMR. When freeze-dried DDase was reacted with highly concentrated G3 (500 mM) for 96 h, the IMS yield increased to 15.8%, but the DP of the α-(1→6)-segment was low [DP = 12.0 with nine α-(1→6)-glucosyl units].

The IMSs produced from G6/G7 and G12 (corresponding to IMS-13/6 and IMS-15/9, respectively) had the estimated DPs of 19.3 and 23.5, respectively (Table 1), and contained α-(1→4)-glucosyl units with average DPs of 6 and 9 at the reducing ends, respectively (Fig. 1). We used IMS-

13/6 as a substrate, for which the α-(1→4)-segment was selectively cleaved by α-amylase (Lang et al., 2020) and converted into a maltodextrin moiety (average DP = 3) to generate an additional IMS (IMS-13/3) with DP = 15.8. The size distributions of the three IMSs were compared with that of the substrate used (Fig. 2C). Chain length of α-(1→4)-segment of each IMS was analyzed by dextran glucosidase digestion (Lang et al., 2020), and maltodextrins corresponding to α-(1→4)-segment were formed (Fig. S3). The IMS structures are shown in Fig. 1, where IMS-13/3 and IMS-13/6 have the same α-(1→6)-segment structure with average DP = 13, and IMS-15/9 has a longer α-(1→6)-segment with average DP = 15. The α-(1→6)-segment contents were 83.3, 69.3, and 63.2% for IMS-13/3, IMS-13/6, and IMS-15/9, respectively.

3.2 Thermal decomposition and water solubility of IMS

The activation energy for amylopectin is higher compared with amylose (Pigłowska et al., 2020). This phenomenon can be explained by its high molecular weight and α-(1→6)-segment content (Liu et al., 2010), suggesting that the α-(1→6)-linked saccharide is more stable than the α-(1→4)-linked saccharide. Therefore, an IMS containing these two segments should be more stable than amylose with a similar size. To investigate the IMS chimeric property, we used TGA to measure the apparent thermal decomposition temperature (TDT) of the IMSs, with amylose and dextran as control saccharides. Under heating in a TGA apparatus in an N_2 atmosphere, IMS-15/9 remained unchanged below 260 °C except for moisture loss, followed by thermal decomposition corresponding to a total weight loss of 89.13% at 500 °C (Fig. 3A). Similar curves were observed for the other samples. The decomposition peak in the differential thermal analysis curve (Fig. 3A) was used to estimate the TDT of each saccharide (Table 2). The TDT of amylose increased with DP, whereas that of dextran did not [Table 2 shows that dextran T10 (DP = 60) and T40 (DP = 250) have lower TDTs than T1 (DP = 7)]. This result is probably due to the low quantities of other glucosidic linkages, such as α-(1→2)- or α-(1→3)-bonds, in the chains of the dextrans T10 and T40 (commercially available samples). A comparison of the TDTs of saccharides with nearly identical DPs [i.e., dextran T3.5 (DP = 20; TDT = 304.7 °C), IMS-13/6 (DP = 19.3; TDT = 304.7 °C), and amylose (DP = 20; TDT = 297.6 °C

(Saavedra-Leos et al., 2015)] shows that the thermal stability of IMS is similar to that of dextran and higher than that of amylose.

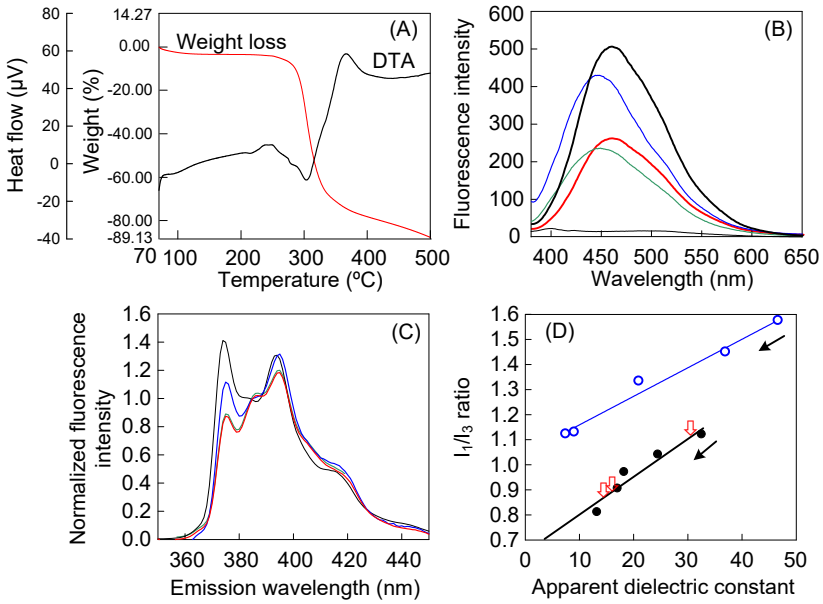

Fig. 3. Characterization of isomaltomegalosaccharide (IMS). **A**, Thermal decomposition of IMS-15/9; DTA, differential thermal analysis. **B**, Emission spectra of 10 μM TNS in water (thin black line) and in 10 mM glucosaccharide; green, IMS-13/3; blue, IMS-13/6; thick black, IMS-15/9; red, G7. **C**, Normalized pyrene emission spectra; black, water containing 1 % (v/v) ethanol (blank); blue, IMS-13/3; green, IMS-13/6; red, IMS-15/9. **D**, Calibration curves for I_1/I_3 *versus* the apparent dielectric constant: polar protic solvents (●, in the direction of the black arrow, methanol, ethanol, 2-propanol, 1-butanol, and 1-hexanol; $Y = 0.015X + 0.647$, $R^2 = 0.922$: Y and X represent I_1/I_3 and apparent dielectric constant, respectively) and polar aprotic solvents (○, in the direction of the black arrow, dimethyl sulfoxide, acetonitrile, acetone, dichloromethane, and tetrahydrofuran; $Y = 0.011X + 1.047$, $R^2 = 0.979$). Red arrows from left to right, IMS-15/9, IMS-13/6, and IMS-13/3 (100 mM for each). Ethanol solution of pyrene was used, and the final concentration of ethanol was 1% (v/v).

299 **Table 2.** Physical properties of isomaltomegalosaccharide (IMS), amylose, and dextran.

Glucosaccharide (DP)	Decomposition temperature (°C)	Water solubility at 25 °C (mg/mL)	K_c by TNS (M^{-1})	I_1/I_3 determined by pyrene[a] (dielectric constant[b]) 100 mM	40 mM	20 mM	K_s for Q3G (M^{-1})	K_s for QC (M^{-1})
IMS								
IMS-13/3 (15.8)	297.1	> 400	14.8	1.12 (31.3)	1.24 (39.5)	1.39 (49.5)	9.0	1.4
IMS-13/6 (19.3)	304.7	> 400	55.2	0.88 (15.8)	0.92 (18.2)	0.95 (20.2)	12.5	1.5
IMS-15/9 (23.5)	305.7	> 400	114	0.87 (15.1)	0.89 (16.2)	0.93 (18.9)	56.3	3.7
Amylose								
G5 (5)			1.9[c]					
G6 (6)			8.8[c]					
G7 (7)			27[c]				6.01	0
Corn (18)		15.5 ± 2.1						
Amylose (20)	279.6[d]							
Synthetic (28)	304.2	10.5 ± 1.5						
Synthetic (600)	309.8	0.52 ± 0.02						
Dextran								
T1 (7)	302.4	> 400		1.29 (42.9)	1.34 (46.2)	1.38 (48.9)	5.73	0
T1.5 (10)				1.25 (40.1)	1.25 (40.2)	1.29 (42.9)	5.86	0
T3.5 (20)	304.7	> 400		1.27 (41.2)	1.28 (42.2)	1.28 (42.2)		
T10 (60)	297.9	> 400		1.31 (44.5)	1.33 (45.5)	1.32 (44.9)		
T40 (250)	299.9	> 400 (swelling)						

300 [a] Pyrene in ethanol solution was added to saccharide sample, where the final concentration of ethanol was 1% (v/v).

[b] Estimated using the standard curve presented in Fig. 3D.

[c] Aoyama et al., 1992.

[d] Saavedra-Leos et al., 2015.

IMS possessed a high water solubility identical to that of short dextran (T3.5; DP = 20), i.e., > 400 mg/mL at 25 °C (Table 2). Large dextran (T40; DP = 250) maintained a high water solubility and became swollen and very viscous. By contrast, amylose with DP = 18–28 exhibited a low solubility of 15–10 mg/mL (Table 2). Long amyloses typically have poor water solubility (Mukerjea & Robyt, 2010) because the crystalline packing of double helices in A- and B-type conformations reduces the binding capacity of water (Naknean & Meenune, 2010). The results obtained indicate that the high aqueous solubility of IMS derives from the α-(1→6)-segment. Hence, our findings elucidate the effect of the α-(1→6)-segment on thermal stability and water solubility, indicating the advantage offered by the chimeric IMS structure.

3.3 Using fluorescent TNS and pyrene to monitor the hydrophobicity of IMS

The hydrophobic interaction between TNS and dextran was reported as undetectable, because the methine groups in a flexible twofold crankshaft-like conformation of dextran are turned toward the bulk water medium (Sundari & Balasubramanian, 1997). However, the α-(1→4)-segment of amylose considerably increases the degree of hydrophobicity, the extent of which depends on the chain length, which generates curved nonpolar surfaces or several helical forms. The hydrophobic interaction is weak between TNS and G3 and not very selective at binding, but it is detectable for maltodextrin with DP of 5 or higher. Perhaps maltodextrins with DP ≥ 5 can undergo an induced-fit adjustment to interact with hydrophobic ligands (e.g., TNS), similar to the hydrophobic cavity of cyclodextrin (Aoyama et al., 1992). The K_cs of G5 (maltopentaose), G6, and G7 have been estimated using TNS to be 1.9, 8.8, and 27 M^{-1}, respectively (Aoyama et al., 1992). These results suggest that IMS possesses hydrophobicity that mainly originates from the α-(1→4)-segment. The K_cs of IMS-13/3, IMS-13/6, and IMS-15/9 were evaluated to be 14.8, 55.2, and 114 M^{-1}, respectively (Fig. S4), as expected (Table 2), and increase in the order of increasing length of the α-(1→4)-segment (average DP = 9 > 6 > 3). The fluorescence intensity of IMS-15/9 was significantly increased, and the maximum wavelength shifted to 467 nm from 447 nm for IMS-13/3 and IMS-13/6 (Fig. 3B), suggesting that the hydrophobic area of IMS-15/9 occupies a more polar environment than of IMS-13/3 and IMS-13/6 (Barel, 1975). The same phenomenon was also observed for G7, where the maximum wavelength was 467 nm (Fig.

3B), which further supports that the high hydrophobicity of IMS-15/9 originates from the α-(1→4)-segment.

Furthermore, the polarity of the IMS hydrophobicity was examined by monitoring the fluorescence spectrum of the complex formed between 0.5 μM pyrene and 100 mM IMS (Fig. 3C), which was used to estimate I_1/I_3 (Table 2). A high I_1/I_3 indicates a high polarity. The I_1/I_3s of IMS-13/3, IMS-13/6, and IMS-15/9 showed that the I_1/I_3 decreased as the length of the α-(1→4)-segment of IMS increased, indicating that the IMS hydrophobicity derives from the α-(1→4)-segment. The α-(1→6)-saccharide dextran (DP = 7–60; 100 mM) possessed larger I_1/I_3 values than 100 mM IMS (Table 2). We measured I_1/I_3 for polar protic and polar aprotic solvents. I_1/I_3 = 0.81–1.12 was measured for polar protic solvents, which contain a hydroxy group (and/or other polar protic groups) that can donate a proton, whereas I_1/I_3 = 1.12–1.57 was measured for polar aprotic solvents that do not contain such groups. The following solvents were investigated: polar protic solvents, methanol (I_1/I_3 = 1.12; dielectric constant = 32.7), ethanol (1.04; 24.6), 2-propanol (0.97; 19.9), 1-butanol (0.91; 17.5), and 1-hexanol (0.81; 13.3); polar aprotic solvents, dimethyl sulfoxide (1.57; 46.7), acetonitrile (1.45; 37.5), acetone (1.33; 20.7), dichloromethane (1.13; 8.93), and tetrahydrofuran (1.12; 7.58). Fig. 3D shows the calibration curves (I_1/I_3 *versus* the dielectric constant) of the polar protic and aprotic solvents, and the calibration curves of the polar protic solvents was used to estimate the IMS dielectric constants (Table 2), because carbohydrates have polar hydroxyl groups. These dielectric constants indicate that the polarities of IMS-13/3, IMS-13/6, and IMS-15/9 are comparable to methanol, 1-butanol, and 1-butanol, respectively. Table 2 shows that the I_1/I_3s of 20 and 40 mM IMS are lower than those of the 20 and 40 mM dextrans, demonstrating that IMS hydrophobicity is maintained at low concentrations. Fluorescence studies using TNS and pyrene indicate that the IMS hydrophobicity mainly originates from the α-(1→4)-segment.

3.4 Solubility enhancement of QC and Q3C by IMS

QC flavonoids are known to have poor water solubility: 4.7 ± 0.4 μM for QC and 156.3 ± 5.5 μM for Q3G at 25 °C in water (both showed pH 6.80). This characteristic derives from the methyl groups and *iso*-pentyl groups in these structures that increase lipophilicity (Crozier et al., 2009), which

results in poor solubility. β-Cyclodextrin or its derivatives have been successfully used to improve the solubility of these flavonoids by forming inclusion complexes (Sun et al., 2008; Pinho et al., 2014). We analyzed the IMS-mediated water solubility of QC flavonoids. A phase solubility diagram assay was employed for this purpose. The solubility curves of Q3G and QC in water were classified as the A_L type (Higuchi & Connors, 1965) for all the IMSs, indicating that the solubility increased with the IMS concentration (Fig. 4). The K_ss for QC and Q3G (Table 2) decreased in the order IMS-15/9 > IMS-13/6 > IMS-13/3, that is, as the length of the α-(1→4)-segment decreased. G7 exhibited lower solubilization of both flavonoids than the IMSs (Fig. 4), probably because of the low water solubility of the G7–Q3G complex and the absence of the formation of a G7–QC complex (Table 2). The same phenomena were observed for the short dextrans T1 (DP = 7) and T1.5 (DP = 10) as for G7. The solubility of Q3G and QC was enhanced by 2.5- and 4.5-fold in the presence of 40 mM IMS-15/9. IMS has a chimeric structure composed of a rigid hydrophobic α-(1→4)-segment and a flexible hydrophilic α-(1→6)-segment. The hydrophobic segment complexes with hydrophobic compound(s), and the hydrophilic segment enhances the water solubility of the complex.

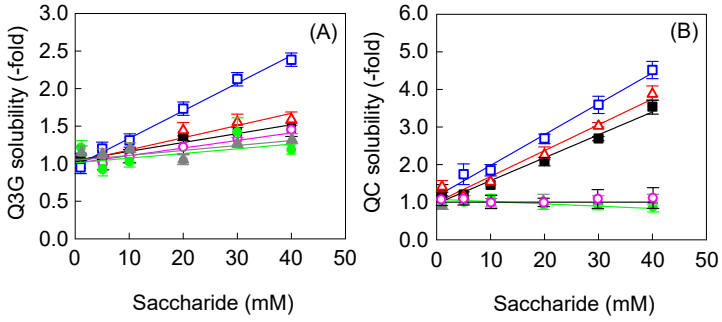

Fig. 4. Phase solubility diagram for solubilization of quercetin-3-*O*-β-glucoside (Q3G) and quercetin (QC) by saccharides. **A**, Q3G; **B**, QC; □, IMS-15/9; Δ, IMS-13/6; ■, IMS-13/3; ○, G7; ●, T1; ▲, T1.5.

The hydrophobicity of IMS mainly originates from its α-(1→4)-segment. However, both the K_c for TNS and K_s for QC flavonoids are considerably higher than those of maltodextrins (Table 2). We cannot completely explain these phenomena, but a ^{1}H-NMR analysis revealed that ethyl red interacted with the anomeric proton of the α-(1→6)-segment in IMS-8/3 (Lang et al., 2014). These results suggest that the high K_c and K_s derive from the α-(1→6)-segment connecting the α-(1→4)- and α-(1→6)-segments.

4. Conclusions

In the present study, we enzymatically synthesized IMSs containing α-(1→4)-segments of various lengths from maltodextrins and investigated the IMS functions. The α-(1→6)-segment of an IMS is hydrophilic and contributes to high water solubility and resistance to thermal decomposition. The α-(1→4)-segment of an IMS can interact with hydrophobic ligands, and interaction depends on the length of α-(1→4)-chain. The IMS chimeric nature, that is, bifunctionality of hydrophilicity and hydrophobicity, enhances the aqueous solubility of compounds with low water solubility (e.g., QC flavonoids), suggesting that IMSs could be extensively applied to industrial fields.

Acknowledgments

We would like to thank Prof. Takayuki Kurokawa (Faculty of Advanced Life Science, Hokkaido University; Sapporo, Japan) for assistance with the TGA analysis. We would like to thank Nihon Shokuhin Kako (Tokyo, Japan) for donating Fujioligo G6 and G7 and Fujioligo G3. This study was partially supported by the Program for Promotion of Basic and Applied Research for Innovations in Biooriented Industry (BRAIN, Japan; Grant Nos. 25001A and 26062B) and the Japan Society for the Promotion of Science KAKENHI (Grant Nos. 17H03801 and 19KK0147). The manuscript received profitable English proof from Elsevier's Author Services.

CRediT authorship contribution statement

Weeranuch Lang: Conceptualization, Investigation, Formal analysis, Writing - original draft. Yuya Kumagai: Formal analysis, Validation. Shinji Habu: Methodology, Formal analysis. Juri Sadahiro: Investigation, Methodology. Takayoshi Tagami: Resources, Supervision. Masayuki Okuyama: Data curation, Resources. Shinichi Kitamura: Supervision, Validation. Nobuo Sakairi: Conceptualization, Supervision. Atsuo Kimura: Writing - review & editing, Resources, Supervision, Funding acquisition, Project administration.

Declaration of Competing Interest

The authors have no conflicts of interest to declare.

References

Allison, S. D., Randolph, T. W., Manning, M. C., Middleton, K., Davis, A., & Carpenter, J. F. (1998). Effects of drying methods and additives on structure and function of actin: Mechanisms of dehydration-induced damage and its inhibition. *Archives of Biochemistry and Biophysics*, *358*(1), 171–181. https://doi.org/10.1006/abbi.1998.0832

Anchordoquy, T. J., Izutsu, K., Randolph, T. W., & Carpenter, J. F. (2001). Maintenance of quaternary structure in the frozen state stabilizes lactate dehydrogenase during freeze – drying. *Archives of Biochemistry and Biophysics*, *390*(1), 35–41. https://doi.org/10.1006/abbi.2001.2351

Aoyama, Y., Otsuki, J. I., Nagai, Y., Kobayashi, K., & Toi, H. (1992). Host-guest complexation of oligosaccharides : interaction of maltodextrins with hydrophobic fluorescence probes in water. *Tetrahedrom Letters*, *33*(26), 3775–3778. https://doi.org/10.1016/0040-4039(92)80022-c

Balasubramanian, D., Raman, B., & Sundari, C. S. (1993). Polysaccharides as amphiphiles. *Journal of the American Chemical Society*, *115*(1), 74–77. https://doi.org/10.1021/ja00054a010

Barel, A. (1975). Fluorimetric study of conformational changes of various α-lactalbumins on agarose carriers. *European Journal of Chemistry*, *473*, 463–473. https://doi.org/10.1111/j.1432-1033.1975.tb09824.x

Buranaboripan, W., Lang, W., Motomura, E., & Sakairi, N. (2014). Preparation and characterization of polymeric host molecules, β-cyclodextrin linked chitosan derivatives having different linkers. *International Journal of Biological Macromolecules*, *69*, 27–34. https://doi.org/10.1016/j.ijbiomac.2014.05.016

Crozier, A., Jaganath, I. B., Clifford, M. N., Crozier, A., Jaganath, B., & Clifford, M. N. (2009). Dietary phenolics : chemistry, bioavailability and effects on health. *Natural Product Reports*, *26*(8), 1001–1043. https://doi.org/10.1039/b802662a

Das, K., Sarkar, N., Das, S., & Bhattacharyya, K. (1995). Fluorescence monitoring of the hydrophobic surface of dextrin using *p*-toluidinonaphthalenesulfonate. *Langmuir*, *11*(13), 2410–2413. https://doi.org/10.1021/la00007a016

Dubois, M., Gilles, A, K., Hamilton, K, L., Rebers, A, P., & Smith, F. (1959). Colorimetric method for determination of sugars and related substances. *Analytical Chemistry*, *28*, 350–356. https://doi.org/10.1021/ac60111a017

Hara, H., Kume, S., Iizuka, T., Fujimoto, Y., & Kimura, A. (2017). Enzymatically synthesized megalo-type isomaltosaccharides enhance the barrier function of the tight junction in the intestinal epithelium. *Bioscience, Biotechnology and Biochemistry*, *82*(4), 629–635. https://doi.org/10.1080/09168451.2017.1398065

Higuchi, T., & Connors, A. (1965). Phase-solubility techniques. *In: Reilly CN, Editor. Advances in Analytical Chemistry Instrumentation. Vol. 4. New York, NY: Interscience*, *4*, 117–212.

Lang, W., Kumagai, Y., Sadahiro, J., Maneesan, J., Okuyama, M., Mori, H., Sakairi, N., & Kimura, A. (2014). Different molecular complexity of linear-isomaltomegalosaccharides and β-cyclodextrin on enhancing solubility of azo dye ethyl red: Towards dye biodegradation. *Bioresource Technology*, *169*, 518–524. https://doi.org/10.1016/j.biortech.2014.07.025

Lang, W., Kumagai, Y., Sadahiro, J., Saburi, W., Sarnthima, R., Tagami, T., Okuyama, M., Mori, H., Sakairi, N., Kim, D., & Kimura, A. (2022). A practical approach to producing isomaltomegalosaccharide using dextran dextrinase from *Gluconobater oxydans* ATCC 11894. *Applied Microbiology and Biotechnology*, *106*, 689–698. https://doi.org/10.1007/s00253-021-11753-6

Liu, P., Yu, L., Wang, X., Li, D., Chen, L., & Li, X. (2010). Glass transition temperature of starches with different amylose / amylopectin ratios. *Journal of Cereal Science*, *51*(3), 388–391. https://doi.org/10.1016/j.jcs.2010.02.007

Mukerjea, R., & Robyt, J. F. (2010). Isolation, structure, and characterization of the putative soluble amyloses from potato, wheat, and rice starches. *Carbohydrate Research*, *345*(3), 449–451. https://doi.org/10.1016/j.carres.2009.11.021

Naknean, P., & Meenune, M. (2010). Review Article. Factors affecting retention and release of flavour compounds in food carbohydrates. *International Food Research Journal*, *34*, 23–34.

Pigłowska, M., Kurc, B., Rymaniak, Ł., Lijewski, P., & Fuć, P. (2020). Kinetics and thermodynamics of thermal degradation of different starches and estimation the OH Group and H_2O content on

the surface by TG/DTG-DTA. *Polymers*, *12*(2), 357. https://doi.org/10.3390/polym12020357

Pinho, E., Grootveld, M., Soares, G., & Heriques, M. (2014). Cyclodextrins as encapsulation agents for plant bioactive compounds. *Carbohydrate Polymers*, *101*, 121–135. https://doi.org/10.1016/j.carbpol.2013.08.078

Saavedra-Leos, Z., Leyva-Porras, C., Araujo-Díaz, S. B., Toxqui-Terán, A., & Borrás-Enríquez, A. J. (2015). Technological application of maltodextrins according to the degree of polymerization. *Molecules*, *20*(12), 21067–21081. https://doi.org/10.3390/molecules201219746

Saburi, W., Mori, H., Saito, S., Okuyama, M., & Kimura, A. (2006). Structural elements in dextran glucosidase responsible for high specificity to long chain substrate. *Biochimica et Biophysica Acta*, *1764*, 688–698. https://doi.org/10.1016/j.bbapap.2006.01.012

Sadahiro, J., Mori, H., Saburi, W., Okuyama, M., & Kimura, A. (2015). Extracellular and cell-associated forms of *Gluconobacter oxydans* dextran dextrinase change their localization depending on the cell growth. *Biochemical and Biophysical Research Communications*, *456*(1), 500–505. https://doi.org/10.1016/j.bbrc.2014.11.115

Shinoki, A., Lang, W., Thawornkuno, C., Kang, H. K., Kumagai, Y., Okuyama, M., Mori, H., Kimura, A., Ishizuka, S., & Hara, H. (2013). A novel mechanism for the promotion of quercetin glycoside absorption by megalo α-1,6-glucosaccharide in the rat small intestine. *Food Chemistry*, *136*(2), 293–296. https://doi.org/10.1016/j.foodchem.2012.08.028

Sun, G., Zhang, X. Z., & Chu, C. C. (2008). Effect of the molecular weight of polyethylene glycol (PEG) on the properties of chitosan-PEG-poly(*N*-isopropylacrylamide) hydrogels. *Journal of Materials Science: Materials in Medicine*, *19*(8), 2865–2872. https://doi.org/10.1007/s10856-008-3410-9

Sundari, C. S., & Balasubramanian, D. (1997). Hydrophobic surfaces in saccharide chains. *Progress in Biophysics & Molecular Biology*, *67*, 183–216. https://doi.org/10.1016/s0079-6107(97)00016-3

Sundari, C. S., Raman, B., & Balasubramanian, D. (1991). Hydrophobic surfaces in oligosaccharides: linear dextrins are amphiphilic chains. *Biochimica et Biophysica Acta*, *1065*, 35–41. https://doi.org/doi: 10.1016/0005-2736(91)90007-u

Suzuki, M., Unno, T., & Okada, G. (1999). Simple purification and characterization of an extracellular

dextrin dextranase from *Acetobacter capsulatum* ATCC 11894. *Journal of Applied Glycoscience*, *46*(4), 469–473. https://doi.org/https://doi.org/10.5458/jag.46.469

Thoma, J. A., Wright, H. B., & French, D. (1959). Partition chromatography of homologous saccharides on cellulose columns. *Archives of Biochemistry and Biophysics*, *85*(2), 452–460. https://doi.org/10.1016/0003-9861(59)90510-7

Yamamoto, K., Yoshikawa, K., Kitahata, S., & Okada, S. (1992). Purification and some properties of dextrin dextranase from Acetobacter capsulatus ATCC 11894. *Bioscience, Biotechnology, and Biochemistry*, *56*(2), 169–173. https://doi.org/10.1271/bbb.56.169

Yamamoto, K., Yoshikawa, K., & Okada, S. (1993). Effective dextran production from starch by dextrin dextranase with debranching enzyme. *Journal of Fermentation and Bioengineering*, *76*(5), 411–413. https://doi.org/10.1016/0922-338X(93)90035-7